Available online at www.sciencedirect.com
ScienceDirect
Geochimica et Cosmochimica Acta 75 (2011) 3803–3814
Geochimica et Cosmochimica Acta
www.elsevier.com/locate/gca

Specific effects of background electrolytes on the kinetics of step propagation during calcite growth

Encarnación Ruiz-Agudo [a,*], Christine V. Putnis [a], Lijun Wang [b], Andrew Putnis [a]

[a] Institut für Mineralogie, Universität Münster, Corrensstrasse 24, 48149 Münster, Germany
[b] College of Resources and Environment, Huazhong Agricultural University, Wuhan, Hubei 430070, China

Received 10 November 2010; accepted in revised form 11 April 2011; available online 20 April 2011

Abstract

The mechanisms by which background electrolytes modify the kinetics of non-equivalent step propagation during calcite growth were investigated using Atomic Force Microscopy (AFM), at constant driving force and solution stoichiometry. Our results suggest that the acute step spreading rate is controlled by kink-site nucleation and, ultimately, by the dehydration of surface sites, while the velocity of obtuse step advancement is mainly determined by hydration of calcium ions in solution. According to our results, kink nucleation at acute steps could be promoted by carbonate-assisted calcium attachment. The different sensitivity of obtuse and acute step propagation kinetics to cation and surface hydration could be the origin of the reversed geometries of calcite growth hillocks (i.e., rate of obtuse step spreading < rate of acute step spreading) observed in concentrated (ionic strength, IS = 0.1) KCl and CsCl solutions. At low IS (0.02), ion-specific effects seem to be mainly associated with changes in the solvation environment of calcium ions in solution. With increasing electrolyte concentration, the stabilization of surface water by weakly paired salts appears to become increasingly important in determining step spreading rate. At high ionic strength (IS = 0.1), overall calcite growth rates increased with increasing hydration of calcium in solution (i.e., decreasing ion pairing of background electrolytes for sodium-bearing salts) and with decreasing hydration of the carbonate surface site (i.e., increasing ion pairing for chloride-bearing salts). Changes in growth hillock morphology were observed in the presence of Li^+, F^- and SO_4^{2-}, and can be interpreted as the result of the stabilization of polar surfaces due to increased ion hydration. These results increase our ability to predict crystal reactivity in natural fluids which contain significant amounts of solutes.

1. INTRODUCTION

The mechanisms by which background ions in solution exert specific effects on the kinetics of growth and dissolution of minerals are just now beginning to be unravelled. Traditionally, the effect of background electrolytes or the "ionic strength" effect (Buhmann and Dreybrodt, 1987) on growth and dissolution rates of minerals has been attributed to changes in solubility. The strong long-range electric fields emanating from the background ions reduce the activity of the ions building the crystal due to charge screening, hence increasing its solubility. Nevertheless, several studies have shown that the dependence of growth or dissolution rates of minerals on ionic strength is not independent of the ionic species producing it (Dove and Czank, 1995; Weaver et al., 2007; Kowacz and Putnis, 2008; Ruiz-Agudo et al., 2009, 2010). Continuum electrostatics models (i.e., those considering the ions as point charges) fail to explain the differential effects exerted by ions having different surface charge densities.

Experimental and computational studies have shown that crystal growth and dissolution rates of sulfates and carbonates are controlled by cation hydration–dehydration dynamics (Pokrovsky and Schott, 2002; Piana et al., 2006). This can be also inferred from the results of the experimental

* Corresponding author. Tel.: +49 0 251 83 36107; fax: +49 0 251 83 38397.
E-mail address: eruiz_01@uni-muenster.de (E. Ruiz-Agudo).

0016-7037/$ - see front matter © 2011 Elsevier Ltd. All rights reserved.
doi:10.1016/j.gca.2011.04.012

study of Dove and Czank (1995) showing that the dissolution rate of sulfate minerals is limited by the water affinity of the cation. tgqcant studies on the effect of solution stoichiometry on the kinetics of calcite growth (Larsen et al., 2010a; Stack and Grantham, 2010) have also revealed that, together with the dehydration of the building units in solution, the kink site configuration, geometry and hydration may have a major influence on ion incorporation and thus on the kinetics of growth. Therefore, any factor affecting cation or surface hydration should alter growth and dissolution rates. In multi-component aqueous solutions the hydration of the crystal building-units as well as the solvent structure and dynamics will be modified with respect to pure water, thus affecting the kinetics of crystal growth and dissolution (Kowacz and Putnis, 2008). These changes arise from effects limited to the local environment around the ion and are associated with the hydration shell(s) of the ions (Collins et al., 2007) and the ions' capacity to "break" or "structure" water (i.e., chaotropic and kosmotropic ions, respectively) (Parsons et al., 2010). This has been long recognized to have an important effect on the crystallization, structure and function of organic macromolecules. However, understanding how ion-induced changes in the solvation environment influences mineral growth and dissolution remains quite challenging.

Some recent research has successfully explained trends in growth and dissolution rates in the presence of different 1:1 electrolytes on the basis of the ability of such electrolytes to modify hydration of the crystal constituting ions (i.e., the building units) (Kowacz and Putnis, 2008; Ruiz-Agudo et al., 2010). Here, we present the results of in situ experimental studies using Atomic Force Microscopy (AFM) to observe the growth of calcite by a spiral growth mechanism from aqueous solutions containing 1:1 ionic salts as background electrolytes to illustrate how the solution composition can affect this process. To our knowledge, this is the first systematic study aimed at elucidating the mechanisms by which different monovalent ions affect calcite growth kinetics.

Calcite cleavage surfaces show two main non-equivalent step orientations, one forming an acute angle with the cleavage surface and the other forming an obtuse angle. These steps have different geometry and hydration. By systematically studying the effect of background electrolytes with different hydration characteristics on the kinetics of propagation of these non-equivalent steps, we can obtain insights into how changes in the solvation environment of both surface and solution species affect calcite growth kinetics.

2. METHODOLOGY

In situ observations and measurements of the $\{1\,0\,\bar{1}\,4\}$ calcite surfaces during growth were performed using a fluid cell of a Digital Instruments Nanoscope III Multimode AFM working in contact mode under ambient conditions ($T = 23$ °C). AFM images were collected using Si_3N_4 tips (Veeco Instruments, tip model NP-S20) with spring constants 0.12 and 0.58 N m^{-1}. Images were analyzed using the NanoScope software (Version 5.31r1). Freshly cleaved calcite surfaces (Iceland spar, Chihuahua, Mexico), ca. $3 \times 3 \times 1$ mm in size, were used as substrates for the AFM experiments. Before each growth experiment, doubly-deionised water (resistivity >18 mΩ cm^{-1}) was passed over the crystal to clean the cleaved surface, as well as to adjust the AFM parameters as described in Arvidson et al. (2006). Growth solutions flowed continuously at ca. 60 mL h^{-1} from a syringe coupled to an O-ring-sealed fluid cell containing the sample crystal. This flow rate is high enough to ensure surface control, in agreement with many of the published AFM experiments that address both calcite dissolution (e.g., Liang et al., 1996) and growth (e.g., Teng et al., 1998). Calcite growth solutions were prepared by adding calculated volumes of $CaCl_2$ and $NaHCO_3$ from 1 M stock solutions, that were prepared by dissolving reagent grade sodium bicarbonate ($NaHCO_3$, Aldrich) and calcium chloride ($CaCl_2{\cdot}2H_2O$, Aldrich) into doubly-deionized water. The precision of added volumes is ±1 μL. The chemical speciation of each solution was determined using the PHREEQC software (Parkhurst and Appelo, 1999) considering the input reservoir and the AFM fluid cell as closed systems (i.e., the amount of CO_2 (g) in the system is negligible for the aqueous speciation calculation). The solution stoichiometry, defined as the ratio of the activities of lattice ions in solution ($a_{Ca^{2+}}/a_{CO_3^{2-}}$), was made equal to ca. 1 by adjusting the amount of $NaHCO_3$ and $CaCl_2$. The supersaturation, Ω, was calculated by $\Omega = IAP/K_{sp}$ where IAP is the ion activity product and K_{sp} the solubility product of calcite ($10^{-8.48}$, phreeqc.dat database) at 25 °C. The solution supersaturation was set at 6.5 and the pH in all experiments was 8.5 ± 0.5. Six 1:1 electrolytes were used as background systems in the in situ AFM growth experiments: NaBr, NaI, $NaNO_3$, NaCl, KCl and CsCl. NaF, LiCl and a 2:1 electrolyte, Na_2SO_4, were also tested, but discarded for any rate measurements as they induced changes in the morphology of the growth spirals. Furthermore, the maximum concentration of NaF under our experimental conditions was limited to 0.47 mM due to the possible precipitation of fluorite (CaF_2). Experiments were performed at ionic strength (IS) of 0.1 and 0.02 (only for NaCl, KCl and CsCl). Table 1 shows experimental conditions for each IS. Solutions were prepared immediately before the experiments, with no time to equilibrate with ambient atmosphere, and flowed over the crystal for less than an hour. During this time interval, the growth rate measurements were performed. The stability of the solutions was checked by analyzing the Ca^{2+} concentration by inductively coupled plasma optical emission spectrometry, ICP-OES (Varian Vista proaxial) at regular time intervals after the preparation of the solutions. In the first 5 h, fluctuations in the Ca^{2+} concentration determined by this

Table 1
Composition of the solutions used in the growth experiments ($\Omega = 6.5$, $a_{Ca^{2+}}/a_{CO_3^{2-}}$ ca. 1 and pH 8.5 ± 0.5).

IS	$[Ca^{2+}]$ (mM)	$[CO_3^{2-}]$ (mM)	[BE][a] (mM)
0.02	0.31	19.00	0
0.10	0.49	19.12	80

[a] BE = background electrolyte.

method were within the error of the measurements, suggesting that the solutions were stable during the progress of the experiments.

3. RESULTS

Immediately on exposure of the calcite (1 0 $\bar{1}$ 4) cleavage surface to water, typical rhombohedral etch pits rapidly formed and were used to establish the crystallographic orientation of the calcite substrate. Closure of the dissolution pits was first observed upon the injection of growth solutions, and further growth proceeded by the advancement of monomolecular (~3 Å) steps. Under the relatively high supersaturation conditions of our experiments ($\Omega = 6.5$), steps mainly originated from islands generated by two-dimensional surface nucleation. To a lesser extent, the formation of growth hillocks was observed having nucleated at screw dislocations (growth spirals) (Fig. 1). We focused our study on these spirals, as information regarding velocity anisotropy of non-equivalent steps on the calcite cleavage plane can be more easily obtained from a detailed study of the growth kinetics of spiral hillocks.

The four step edges observed on {1 0 $\bar{1}$ 4} faces during growth and dissolution under normal conditions are parallel to $[\bar{4}\,4\,1]_+$, $[4\,8\,\bar{1}]_+$, $[\bar{4}\,4\,1]_-$ and $[4\,8\,\bar{1}]_-$ directions (Fig. 2a). The subscripts (+ or −) follow the convention used by Paquette and Reeder (1995). These steps are bonded by alternating Ca^{2+} and CO_3^{2-} ions. The structurally equivalent $[\bar{4}\,4\,1]_-$ and $[4\,8\,\bar{1}]_-$ steps are acute and intersect the bottom of the etch pit at an angle of 78°, while $[\bar{4}\,4\,1]_+$ and $[4\,8\,\bar{1}]_+$ steps are obtuse and intersect the bottom of the etch pit at an angle of 102° (Hay et al., 2003). Hillocks grown around screw dislocations exhibited a polygonized pyramidal geometry and are formed by growth layers each bounded by two obtuse and two acute step edges (Fig. 2b).

Measurements of geometric relationships of the spiral growth hillocks were made from sequential images scanned in the same direction. From these measurements, the absolute growth velocities of obtuse (v_+) and acute (v_-) steps were determined as in Larsen et al. (2010a,b). The length x and the angles ϕ and γ (defined in Fig. 3), as well as the time lapse, t, between AFM images, can be used to calculate the growth velocities for the obtuse and acute steps using the equations:

$$v_+ = \frac{\sin\left(\frac{\phi+\gamma}{2}\right)}{t} \cdot x$$

$$v_- = \frac{\sin\left(\frac{\phi-\gamma}{2}\right)}{t} \cdot x$$

Average values of v_+, v_- and ϕ and experimental uncertainties for the different experiments performed are shown in Tables 2 and 3. At high ionic strength (0.1), obtuse

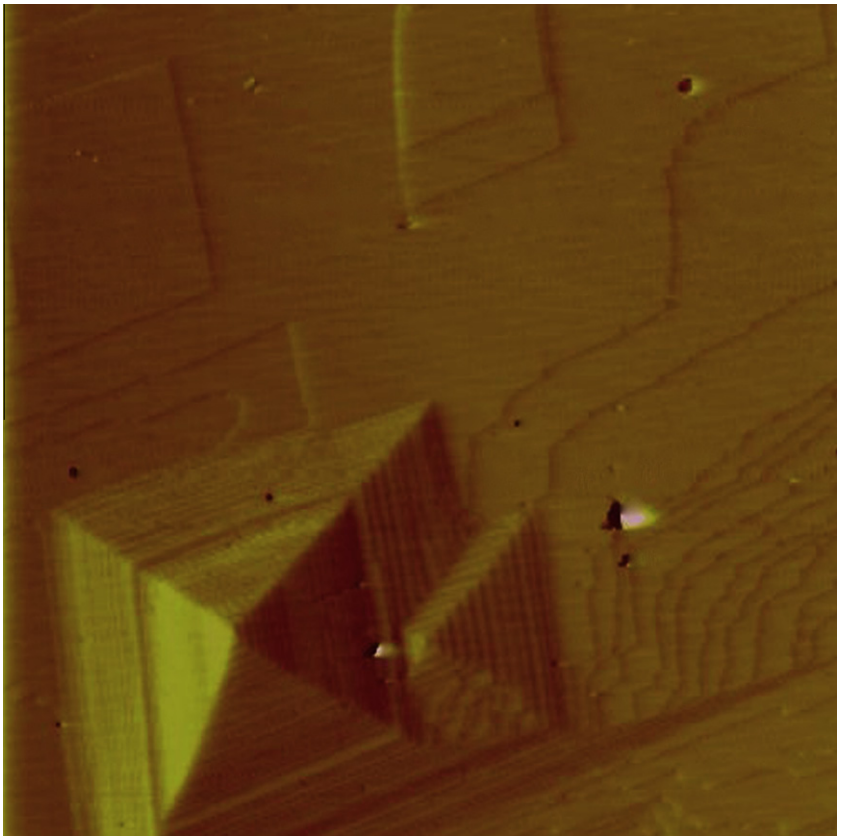

Fig. 1. AFM deflection image of a calcite cleavage surface after the injection of a growth solution ($\Omega = 6.5$, IS = 0.02 – NaCl, $a_{Ca^{2+}}/a_{CO_3^{2-}}$ ca. 1 and pH 8.5 ± 0.5). Coexistence of 2D nuclei and spiral growth is observed.

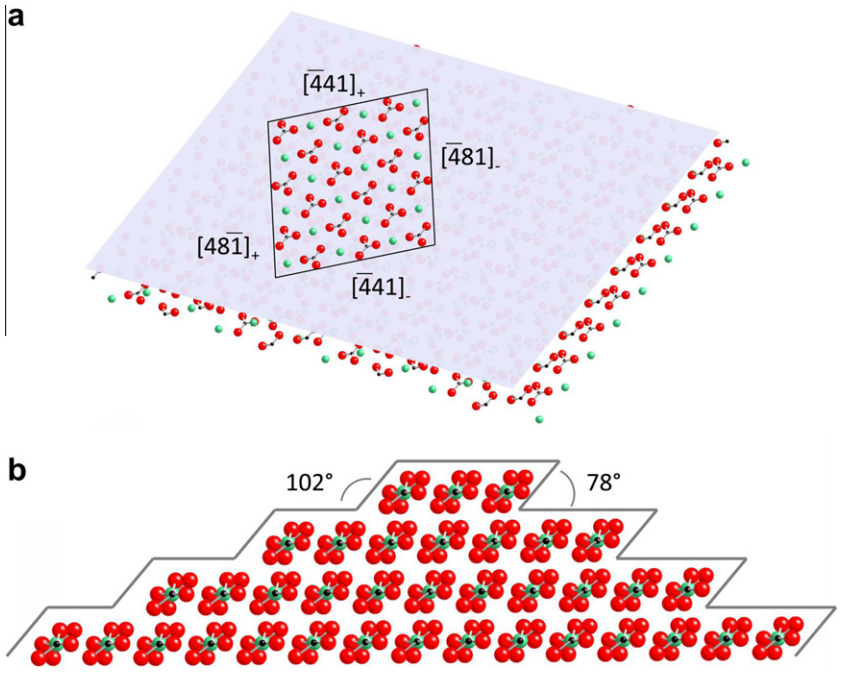

Fig. 2. (a) Normal view of the atomic arrangements in the cleavage plane of calcite. (b) Sketch showing a cross-section of a growth hillock, with the obtuse and acute edges delimiting the layers.

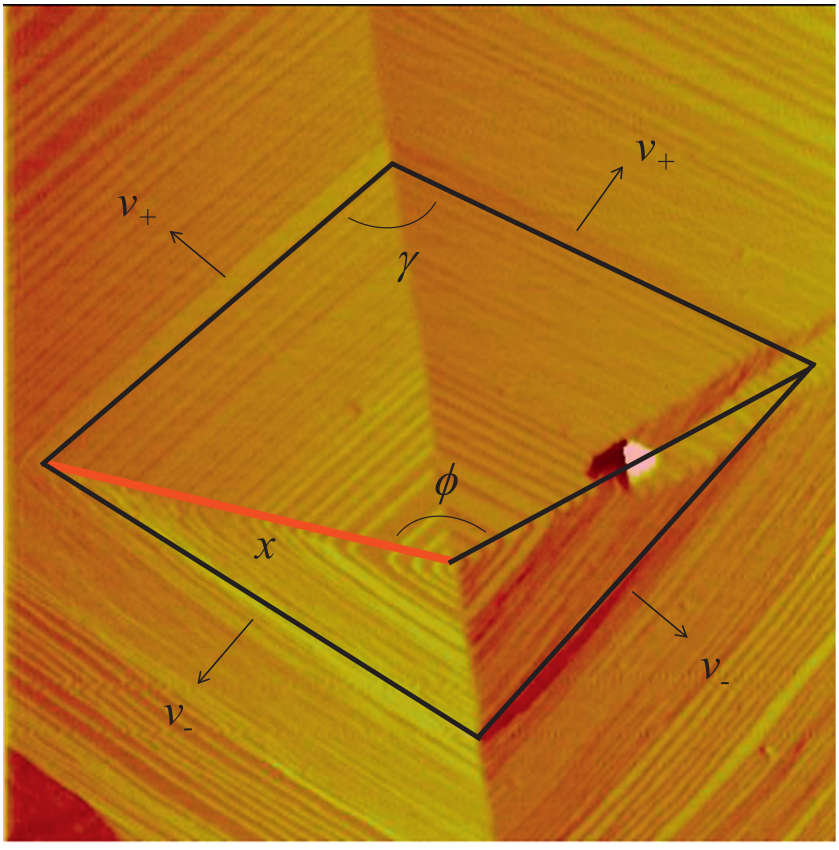

Fig. 3. Geometric relationships of growth spirals (modified from Larsen et al., 2010a,b) used for the calculation of step propagation velocities.

and acute step spreading rates were found to increase in the order $NaCl < NaI < NaBr < NaNO_3$ for sodium bearing salts and $NaCl < CsCl < KCl$ for chloride bearing salts (Fig. 4). Absolute rates ($v_+ + v_-$) were also calculated from

Table 2
Step spreading rates (v/nm s^{-1}) on calcite cleavage surfaces and angle between obtuse steps (ϕ, °) for different background electrolytes at IS = 0.1.

	v_+ (nm s^{-1})		v_- (nm s^{-1})		$v_+ + v_-$ (nm s^{-1})		v_+/v_- (nm s^{-1})		ϕ	
	Avg	Std	Avg	Std	Avg	Std	Avg	Std	Avg	Std
NaCl	8.60	0.82	2.45	0.34	11.05	0.75	3.51	0.75	139.6	1.0
CsCl	10.48	0.64	11.09	1.05	21.57	2.94	0.95	0.26	185.6	6.2
KCl	13.45	1.72	12.24	1.73	25.69	3.69	1.10	0.44	176.2	2.7
NaI	7.89	0.48	2.96	0.11	10.85	0.83	2.67	0.86	140.1	3.8
NaBr	9.51	0.99	3.29	0.44	12.80	1.38	2.89	0.27	139.7	2.2
$NaNO_3$	18.09	1.73	4.22	0.45	22.31	2.18	4.29	0.70	120.2	2.6

Table 3
Step spreading rates (v/nm s^{-1}) on calcite cleavage surfaces and angle between obtuse steps (ϕ, °) for different background electrolytes at IS = 0.02.

	v_+ (nm s^{-1})		v_- (nm s^{-1})		$v_+ + v_-$ (nm s^{-1})		v_+/v_- (nm s^{-1})		ϕ	
	Avg	Std	Avg	Std	Avg	Std	Avg	Std	Avg	Std
NaCl	7.78	0.58	2.84	0.61	10.62	1.20	2.74	0.80	137.3	6.4
CsCl	6.15	1.00	3.87	0.61	10.02	1.61	1.59	0.51	157.7	1.9
KCl	4.86	0.55	4.39	0.68	9.25	1.23	1.11	0.30	168.9	4.7

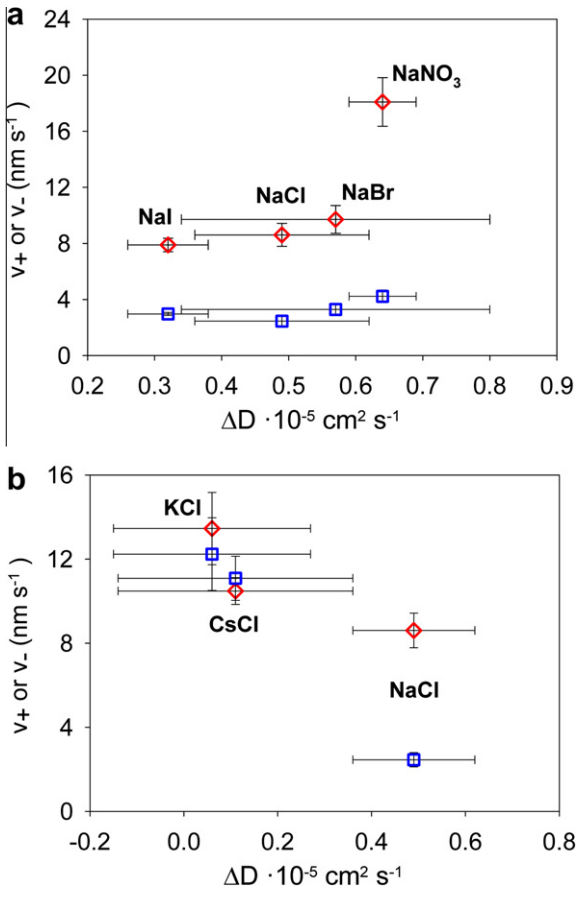

Fig. 4. Obtuse (v_+, ◇) and acute (v_-, □) step propagation velocities at IS = 0.1 in different background salts as a function of difference in the diffusion coefficients of ionic salt constituents (ΔD): (a) sodium-bearing and (b) chloride-bearing salts.

these data and are shown in Table 2 and Fig. 5, and at IS 0.1 showed the same trends as individual step advancement velocities. The ratio v_+/v_- decreased in the order $NaNO_3$ > NaCl ≈ NaBr ≈ NaI > KCl ≈ CsCl (Table 2, Fig. 5). In the presence of KCl and CsCl, parity or even reversal in the spreading rate of non-equivalent steps (i.e., $v_+ \leqslant v_-$) was clearly observed at IS 0.1, leading to hillock morphologies with "unusual" geometric relationships (Fig. 6). At low ionic strength (0.02) (Fig. 7), no significant differences were found in acute step advancement rates for the chloride-bearing salts tested. Obtuse step velocities decreased in the order NaCl > CsCl ≈ KCl.

Some of the background electrolytes tested induced changes in the morphology of growth spirals (Fig. 8), and therefore experiments performed in the presence of these salts were not used for growth rate measurements. When LiCl was used as a background salt, a new step edge developed roughly parallel to [0 1 0] (Fig. 8a and d). In the presence of Na_2SO_4 (IS 0.1), growth hillocks lost their characteristic rhombohedral shape, and became elongated, acquiring more or less an elliptical or tear-shape appearance (Fig. 8b and d). This seems to be the result of the development of new straight edges parallel to [$\bar{4}$ 2 1], i.e., the elongation direction. Similar changes, although to a lesser extent, were observed in the presence of 0.3 mM NaF (Fig. 8c and f). These effects are ascribed to the presence of Li^+, SO_4^{2-} and F^-, as they were not observed in other Cl- or Na-bearing solutions

4. DISCUSSION

4.1. Rate-limiting processes in acute and obtuse step propagation: carbonate-assisted incorporation of calcium

The kinetics of crystal growth is ultimately determined by the frequency of attachment of building units to the

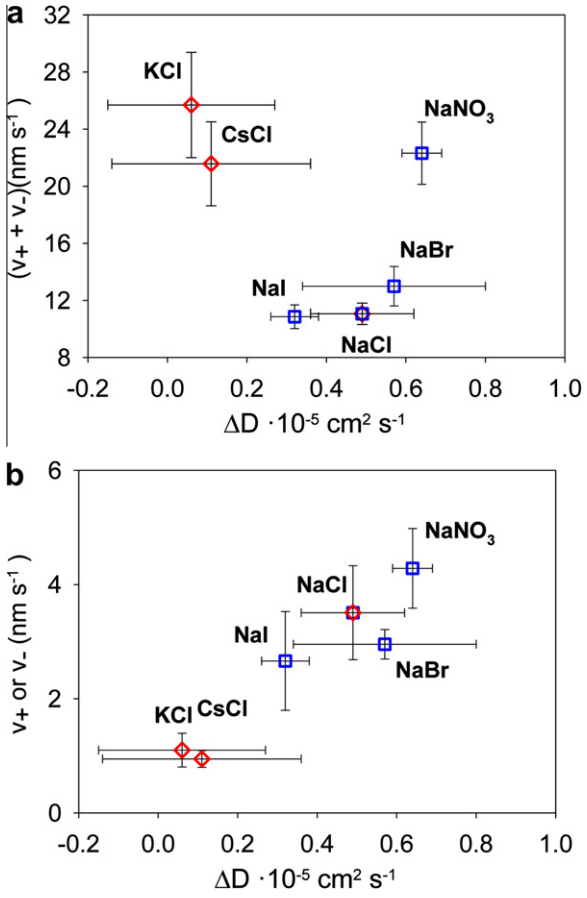

Fig. 5. (a) Overall step advancement rate and (b) obtuse to acute step spreading rate ratio for chloride-bearing (◇) and sodium-bearing (□) electrolytes (IS = 0.1).

crystal. This attachment takes place mainly at kink sites, which are surface sites in which the number of bonds that coordinate the ions building the crystal at that site is half that of the same ions in the bulk crystal structure. During growth, new kinks are formed by random attachment of growth units to a complete step edge. Differences in the rate of kink formation (i.e., one dimensional nucleation) and spreading and thus on the kinetics of step advancement observed for calcite acute and obtuse steps are due to the differential rates of adsorption of Ca^{2+} ions on these steps. This process is thought to be governed by diffusion of the ion through the bulk and interfacial water and dehydration of the aqueous ions as well as the corresponding kink sites at the surface (Stack and Grantham, 2010).

At room temperature, sparingly soluble minerals such as calcite have low kink-site density and thus the process of kink nucleation should contribute considerably to the kinetics of step propagation (De Yoreo et al., 2009). In fact, one dimensional kink nucleation may be limited on specific crystal surfaces by diffusion of the ions through the interfacial water and become the growth rate limiting step. As shown by molecular dynamic simulations for the case of barite, nucleation is limited by a kinetic barrier that prevents the cation from approaching the crystal surface, and is related to the reorganization of the water molecules on the crystal surface and around the ion when it is approaching the surface (Piana et al., 2006). This barrier is expected to have a stronger impact in the case of calcium compared to barium, as strongly hydrated ions, such as Ca^{2+}, will find higher diffusion resistance than weakly hydrated ions, such as Ba^{2+}, in their migration towards the mineral surface. As shown by density functional theory calculations, water binds more strongly to acute steps than to obtuse steps (Lardge et al., 2010). Therefore, for an obtuse step this effect is expected to be less important as its solvation is weaker and thus hydration water will represent a smaller resistance towards ion diffusion to the crystal surface. It should be noted that the calculations by Lardge et al. (2010) refer to water binding in vacuo and in solution, water–water interactions could make a difference. Nevertheless, and due to the lack of other data regarding hydration of the non-equivalent steps, we consider that these calculations may represent a good approximation. In fact, atomistic simulations have shown that the creation of a kink site by attaching a building unit at a step edge requires four times more energy in the case of acute steps than obtuse steps (de Leeuw et al., 2001), which could be related to the above mentioned differences in water binding strength between non-equivalent steps. Thus, changes in the diffusion resistance are expected to have less impact on the spreading rate of obtuse steps.

The recent work by Larsen et al. (2010a) and Stack and Grantham (2010) has shown that the velocity maximum for acute steps occurs at $a_{Ca^{2+}}/a_{CO_3^{2-}} < 1$. This indicates that higher relative activity of CO_3^{2-} ions is required to accelerate the growth of acute steps (compared to obtuse steps, where the maximum velocity is reached at $a_{Ca^{2+}}/a_{CO_3^{2-}} \geqslant 1$). Considering that calcium ions dehydrate at slower rates than carbonate ions (rate of water exchange of aqueous calcium and carbonates ions, $6–9 \times 10^8$ and $2 \times 10^9\ s^{-1}$, respectively, Stack and Grantham, 2010) one can conclude that cation dehydration in solution is not the only parameter controlling the kinetics of step advancement. As stated before, kink nucleation may be also rate-limiting. For nucleation to occur, both cation and anion have to adsorb at the calcite surface. Piana et al. (2006) showed for the case of barite that cation adsorption on the surface is thermodynamically unfavourable. However, in the presence of anions, the crystal surface facilitates the formation of ion pairs upon diffusion of the cation through the solution. This assists cation attachment to the surface and, as a consequence, makes the process thermodynamically more favourable. It appears that the situation for calcite is somewhat different. Calcium shows no tendency to associate with the flat cleavage surface in the absence of a previously deposited carbonate anion (Raiteri et al., 2010). The carbonate anion does not show any preference between being adsorbed at the flat surface or migrating into the bulk (Raiteri et al., 2010). Also, the $CaCO_3$ neutral ion pair prefers to be solvent separated on the flat surface rather than adsorbed (Raiteri and Gale, 2010). This implies that surface nucleation on calcite is less favourable than on barite, and that the carbonate cannot help to desolvate the cation on a flat surface (although this may not be true for

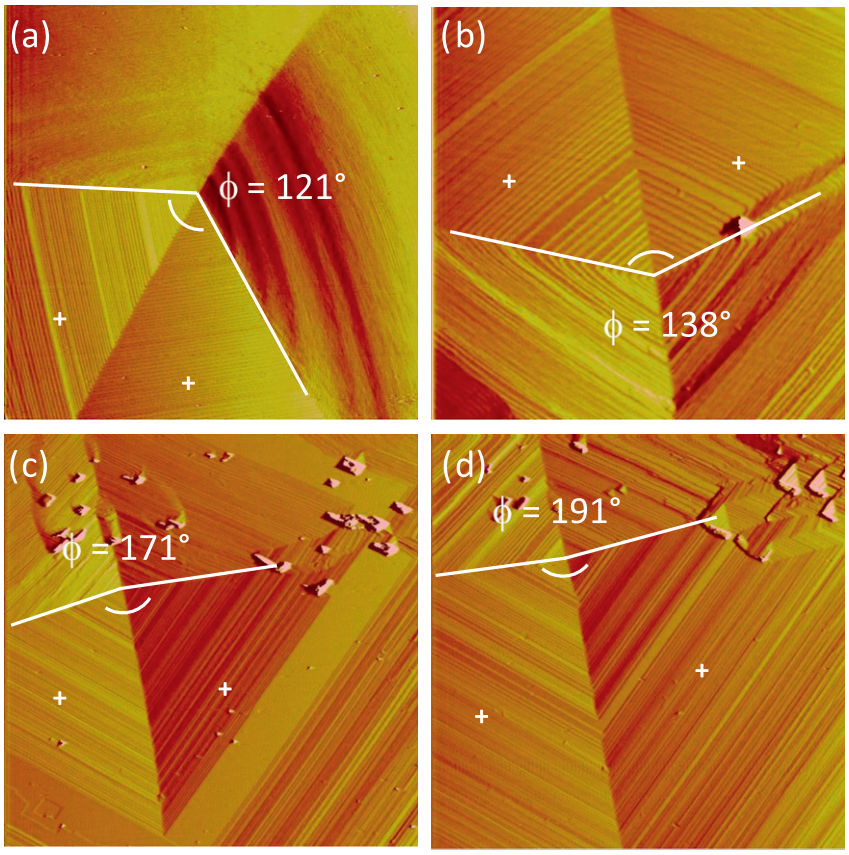

Fig. 6. AFM deflection images of hillocks grown around screw dislocations in supersaturated solutions of $a_{Ca^{2+}}/a_{CO_3^{2-}}$ ca. 1, $\Omega = 6.5$ and IS 0.1 of different background electrolytes: (a) $NaNO_3$, (b) NaCl, (c) KCl and (d) CsCl. The measured value of the angle ϕ is indicated in the images.

bicarbonate). However, this could well happen at kinks. Although currently there are no computational studies that have explored whether carbonate or bicarbonate ions may facilitate calcium attachment at kinks and therefore increase the rate of acute step advancement, this scenario would be in agreement with the fact that the maximum spreading rate of calcite acute steps at a fixed supersaturation is achieved in the presence of an excess of carbonate ions (i.e., $a_{Ca^{2+}}/a_{CO_3^{2-}} < 1$) (Larsen et al., 2010a; Stack and Grantham, 2010).

4.2. Effect of background electrolytes on the spreading rate of acute and obtuse steps

The theoretical considerations above provide a framework for the rationale of the observed effect of the different background salts on the kinetics of calcite growth. As explained, acute step propagation seems to be limited by formation of kink sites and, in particular, by calcium attachment at the surface. This requires dehydration of the oppositely charged carbonate at the surface, and thus changes in the hydration environment of the carbonate group at the surface due to the presence of oppositely charged background cations will affect the kinetics of creation of new attachment sites and calcium incorporation rates. When electrolytes are present in the growth solution, water molecules around building units (either in solution or at the surface) are stabilized compared to pure water due to the electrostatic attraction between water dipoles aligned around the building units and counter ions in solution. However, the formation of ion-pairs will reduce the ability of salts to stabilize water of hydration. The closer the ions constituting the background salt, the more screened are their electric fields and consequently the electrostatic influence on solvation water diminishes. In Fig. 4a, etch pit spreading rates were plotted against the difference in the diffusion coefficients of the ionic salt constituents (ΔD, Table 4). As explained in Ruiz-Agudo et al. (2010), this parameter is a proxy of ion separation in solution. The rate of step advancement was found to decrease in the order KCl > CsCl > NaCl, which correlates well with decreasing ion pairing in solution and thus with the predicted increase in surface carbonate hydration.

At high IS (0.1), similar trends for the different background cations are found for obtuse steps (Fig. 4a). Due to the weaker hydration of these steps, nucleation is not expected to be the limiting factor for step spreading, and in fact, this is reflected in the weaker dependence of obtuse step spreading upon ΔD of chloride-bearing salts. Once nucleation has occurred, step growth will be governed by electrostatics and should be hampered by the presence of water molecules surrounding the building units (Kowacz

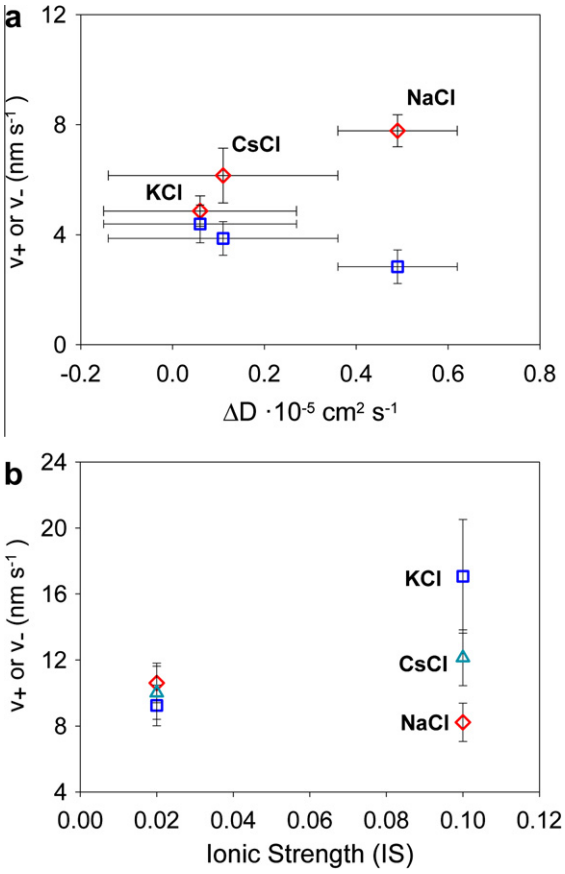

Fig. 7. (a) Obtuse (v_+, ◇) and acute (v_-, □) step propagation velocities at IS = 0.02 in different chloride-bearing salts as a function of difference in the diffusion coefficients of ionic salt constituents (ΔD). (b) Overall step advancement rate as a function of ionic strength for different chloride-bearing salts.

and Putnis, 2008). As calcium ions dehydrate more slowly than carbonate ions, the kinetics of the former will determine the rate of step advancement, when it is not limited by kink nucleation. Considering that background anions will determine solvent structure around Ca^{2+} cations, the most significant differences in the obtuse step advancement would be expected in the presence of different sodium-bearing salts. As seen in Fig. 4b, the rate of step propagation increases with ΔD, and thus in the order NaCl ≈ NaI < NaBr < $NaNO_3$. As in the case of calcite dissolution (Ruiz-Agudo et al., 2010), this trend contrasts with that observed for barite (Kowacz and Putnis, 2008). Following the same arguments as those used in comparing the effects of background electrolytes on the dissolution of barite and calcite (Ruiz-Agudo et al., 2010), this apparent inconsistency may be explained by considering the overall change in entropy of the system upon growth. During crystallization, two entropic effects must be taken into account: there is a decrease in disorder of the crystal building units as well as an increase in disorder of the water molecules when the building units are incorporated into the crystal and they can no longer induce ordering of the water molecules around them. This latter effect is particularly important if the ions are small and highly charged. Ca^{2+} is much more strongly hydrated than Ba^{2+} and its hydration causes significant order of the solvent molecules around it. Therefore, the overall entropy change is higher for calcite than barite. The stabilization of the hydration water by the presence of background salts augments the favourable entropic effect upon calcite growth relative to barite, thus increasing the overall change in entropy of growth. A weaker dependence of the rate of acute step propagation on ΔD of sodium-bearing salts supports the hypothesis that the dehydration of carbonate surface sites, and not the desolvation of cation in solution, could be the main factor controlling the spreading rate of acute steps.

At low ionic strength (0.02), obtuse step velocities weakly decreased with decreasing ion separation in solution and thus in the order NaCl > CsCl ≈ KCl (Fig. 7a). However, differences in acute step advancement rate for the chloride-bearing salts tested were within experimental error. The fact that at low IS the velocity of obtuse step propagation decreased with increasing ion pairing and its higher sensitivity (compared to acute step spreading rate) to separation of background ions suggests that ion-specific effects at this low electrolyte concentration may be mainly related to changes in the solvation environment of ions in solution. Surface hydration does not seem to be significantly altered by the presence of background ions, possibly due to the low percentage of the surface covered by these ions. The effect of increasing salt concentration on step advancement rate is also electrolyte-dependent (Fig. 7b), with $v_+ + v_-$ remaining essentially unaffected in NaCl solutions and $v_+ + v_-$ increasing with KCl and CsCl concentration. This reflects the fact that, with increasing electrolyte concentration, the surface area affected by background ions will be higher and thus stabilization of surface water by weakly paired salts (i.e., NaCl) will become increasingly important in determining step spreading rates.

4.3. Reversed geometries of calcite growth hillocks induced by the presence of background electrolytes

To summarize, our results show that overall calcite growth rates increase with increasing hydration of calcium in solution (i.e., increasing ΔD and thus ion separation in solution for sodium-bearing salts) and with decreasing hydration of the carbonate surface site (i.e., decreasing ΔD and thus ion separation in solution for chloride-bearing salts) (Fig. 5a). The relative sensitivity of obtuse and acute step propagation kinetics to these processes (cation and surface hydration) could be the origin of the observed reversed geometries calcite growth hillocks (i.e., $\phi > 180°$). This can be better understood by looking at the ratio v_+/v_- (Fig. 5b). This ratio will determine the angle ϕ of the growth spirals (Fig. 6): for $v_+/v_- > 1$, $\phi < 180°$; for $v_+/v_- \approx 1$, $\phi \approx 180°$ and $v_+/v_- < 1$, $\phi > 180°$. Parity or even reversal in the non-equivalent growth step velocity (i.e., $v_+ \leqslant v_-$) was not found during growth in NaCl, NaBr, NaI and $NaNO_3$ bearing solutions at $a_{Ca^{2+}}/a_{CO_3^{2-}} = 1$ (this work and Stack and Grantham, 2010). However, this phenomenon has been observed at $a_{Ca^{2+}}/a_{CO_3^{2-}} = 1$ under conditions of decreased hydration of

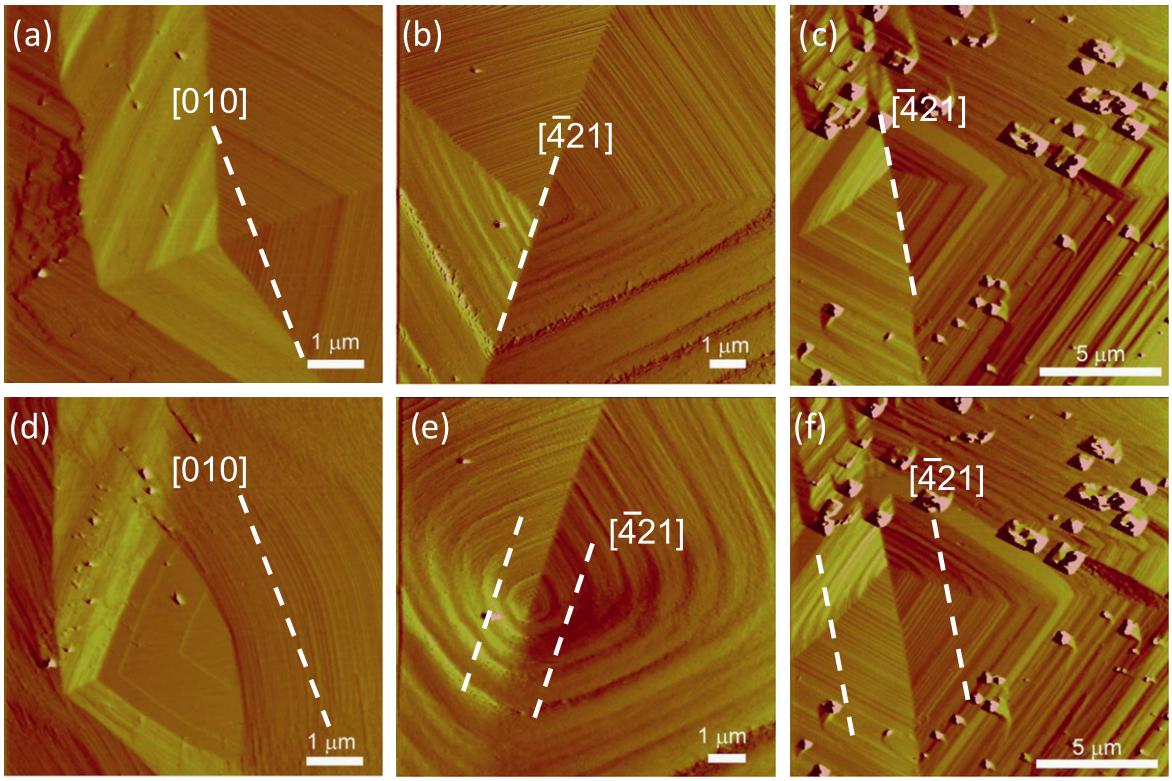

Fig. 8. AFM deflection images of hillocks grown around screw dislocations in supersaturated solutions of $a_{Ca^{2+}}/a_{CO_3^{2-}}$ ca. 1 and $\Omega = 6.5$. Images (a) and (b) are growth from solutions containing NaCl as the background electrolyte (IS 0.1). Images (d) and (e) show the same spirals in (a) and (b), respectively, after changing the background electrolyte for (d) LiCl (IS 0.1) and (e) Na_2SO_4 (IS 0.1). (c) Growth hillock formed in a growth solution containing NaCl (IS 0.02) and (e) the same spiral after adding 0.3 mM NaF to the growth solution.

carbonate surface sites in the presence of background electrolytes (as observed in this work in the presence of KCl and CsCl) or low $a_{Ca^{2+}}/a_{CO_3^{2-}}$ (Stack and Grantham, 2010), probably as a result of increased carbonate-assisted attachment. Both processes could accelerate kink nucleation at acute steps, thus (according to our model) increasing the velocity of propagation of such steps relative to obtuse steps. This would explain the value of $\phi \approx 180°$ reported at $a_{Ca^{2+}}/a_{CO_3^{2-}} = 1$ in recent experiments performed in KCl bearing solutions (Larsen et al., 2010a,b). Reversed morphologies in calcite growth hillocks were first reported by Teng et al. (1999) in NaCl bearing solutions at $a_{Ca^{2+}}/a_{CO_3^{2-}} = 1$ and near-equilibrium conditions (i.e., low supersaturation). These authors claimed that growth modifying effects of impurities were the origin of these morphologies. However, it seems unlikely that impurity pinning by Mg, Sr or Ba (major impurities found in the reagents used in their experiments) was the source of these reversed geometries observed at low supersaturation, as these ions have distinct preferences for acute (Mg^{2+}) or obtuse (Sr^{2+}, Ba^{2+}) step orientation (Paquette and Reeder, 1995; Reeder, 1996; Davis et al., 2004) and, therefore, pinning and reduction of both acute or obtuse step spreading rate should occur. Again, it could be argued that the rate of obtuse step propagation may be more sensitive to a reduction in the activity of calcium in solution than in the case of the acute steps. This is in agreement with the hypothesis presented in this paper regarding obtuse step advancement being mainly affected by the "availability" of calcium in solution for its attachment to a kink site, while acute step advancement seems to be controlled by kink-site nucleation and, ultimately, by the hydration of the carbonate surface. At low supersaturation, the decrease in the spreading rate of obtuse steps due to the reduction in the calcium availability could even overcome the expected increase in obtuse step spreading rate due to the effect of KCl on the hydration of the carbonate surface site. Furthermore, as the background anion will determine the hydration environment around calcium, no dramatic differences should be expected in the case of KCl or NaCl. However, because KCl is more

Table 4
Difference in the diffusion coefficients of ionic salt constituents (ΔD) (Koneshan et al., 1998).

	$\lvert\Delta D\rvert$ (10^{-5} cm^2 s^{-1})	
	Avg	Std
NaCl	0.49	0.13
CsCl	0.11	0.25
KCl	0.06	0.21
NaI	0.32	0.06
NaBr	0.57	0.23
$NaNO_3$	0.64	0.05

ion-paired than NaCl in solution and thus reduces the stabilization of the hydration shell of calcium, a reverse trend in the growth rate (i.e., NaCl > KCl) could be found at low supersaturation. This latter effect seems to be compensated by the higher availability of calcium at high supersaturation and thus it was not observed in our study. Therefore, this discussion highlights the need for using high enough supersaturations in experimental studies aimed at elucidating ion-specific effects, in order to separate such effects from those purely related to the saturation state of the solution.

4.4. Effect of F^-, SO_4^{2-} and Li^+ on growth hillock morphology: surface stabilization due to increased hydration

Changes in the morphology of growth features on calcite cleavage surfaces in the presence of NaF and Na_2SO_4 were previously reported by Vavouraki et al. (2008, 2010). They suggested F^- and SO_4^{2-} incorporation on specific sites of the calcite surface as the most likely cause of the change in growth morphology. Our observations suggest that the morphological changes could be the result of the development of new straight edges parallel to [$\bar{4}$ 2 1]. In the presence of Li^+, a similar effect was observed, with the development in the growth spirals of a new step edge parallel to [0 1 0]. The influence of lithium on calcite macroscopic growth morphology was first described by Rajam and Mann (1990). These authors suggested that Li^+ may be accommodated in the interstices between carbonate ions on the dipolar (0 0 0 1) face, partially neutralizing the dipole moment of this face which is thus stabilized. This would lead to the development of new step edges parallel to [0 1 0] on calcite growth hillocks. A similar effect has been also observed during calcite dissolution in the presence of lithium (Ruiz-Agudo et al., 2010).

Nevertheless, changes in growth morphology may not be solely due to specific interactions between ions and mineral surfaces. The [$\bar{4}$ 2 1] and [0 1 0] directions correspond to the intersection of the {0 1 $\bar{1}$ 2} and {0 0 0 1} forms with the cleavage rhombohedron, respectively. These faces are polar and consist of alternate layers of Ca^{2+} and CO_3^{2-} ions in successive planes. Thus, they are not stable when calcite nucleation and growth takes place in pure solutions. As explained above, the presence of background ions tends to stabilize water molecules in ion hydration shells and at the crystal surface. Increasing ion hydration reduces both repulsive interactions between ions of the same charge and attractive interactions between ions of opposite charges (Kowacz and Putnis, 2008; Ruiz-Agudo et al., 2010). Thus, polar faces will be stabilized while non-polar faces should be less stable in electrolyte solutions. Although (0 1 $\bar{1}$ 2) and (0 0 0 1) faces are not stable under normal growth conditions, both are frequently observed in biomineralized calcite (see Duffy and Harding, 2004 and refs therein). This suggests that "simple" inorganic species may have similar effects on calcite growth morphology at the atomic scale as more complex organic macromolecules and thus, inorganic ions could be used to control crystal growth as well as providing analogues in the study of mineral growth in biological systems.

4.5. Effect of background electrolytes on calcite step propagation and the kink-limited growth model

Some of the observations presented above could be interpreted in terms of the recently proposed kink-limited growth model, which considers that non-incorporating ions compete with crystal building units for attachment at kink sites (De Yoreo et al., 2009). Small ions such as sodium or chloride can approach closer to the surface groups than larger ones, and thus the electrostatic interactions among them will be stronger; these ions will therefore effectively compete with building units for attachment at kink sites, and their presence in solution will result in a decrease in the step spreading rate. Also, for a similar ionic size, ions which are less paired in solution will have their charges less screened and their interaction with surface groups will be stronger. This could explain why spreading rates are slightly slower in CsCl solutions than in KCl solutions, despite the larger ionic radius of Cs^+ compared to K^+. However, differences in sensitivity of obtuse and acute step velocity towards ionic radius of background competing ions as well as the fact that the maximum spreading rate of calcite acute steps at fixed supersaturation is observed at $a_{Ca^{2+}}/a_{CO_3^{2-}} < 1$ are more difficult to explain within the framework of the kink-limited growth model. Therefore, we consider that anion-assisted desolvation remains the most suitable explanation for these observations. Unfortunately, the validity of these models cannot be unequivocally established experimentally, although molecular dynamic simulations may shed more light on the origin of these ion-specific effects. This is, however, beyond the scope of this paper.

5. CONCLUSIONS

The results of this work suggest that the rate of dehydration of carbonate surface sites for cation attachment and subsequent kink nucleation controls the velocity of acute step propagation in calcite cleavage planes. This rate can be altered in the presence of background cations in solution. However, dehydration of calcium ions in solution seems to be rate-limiting for the spreading of obtuse steps. Changes in cation hydration in solution will occur in the presence of different background anions. In our study, overall calcite growth rates increase with increasing hydration of calcium in solution (i.e., increasing ion separation in solution of sodium-bearing salts) and with decreasing hydration of the carbonate surface site (i.e., increasing ion-pairing of chloride-bearing salts). According to our model, kink nucleation at acute steps could be promoted by increasing the relative amount of carbonate ions in solution, as they may assist calcium attachment to complete steps, therefore increasing the spreading rate of acute steps relative to obtuse steps. Changes in growth hillock morphology were observed in the presence of F^-, SO_4^{2-} and Li^+ and could be ascribed to stabilization of polar (0 1 $\bar{1}$ 2) and (0 0 0 1) faces due to increased hydration. These forms are commonly found in biomineralized calcite, suggesting that relatively simple inorganic ions may have similar effects on mineral growth at the atomic scale as more complex organic molecules. The conclusions of this

study increase our ability to predict crystal reactivity in fluids in natural systems, which often contain significant and variable amounts of solutes. Our findings suggest a high sensitivity of relative rates of obtuse and acute step advancement to small differences in the solvation environment of ions in solution and at the mineral surface. This leads to the hypothesis that the uptake of minor and trace metals by calcite, which has been shown to be highly site specific, can be selectively modified by changing the hydration characteristics of the growth fluids.

ACKNOWLEDGEMENTS

This work has been financially supported by the EU Initial Training Network Delta-Min (Mechanisms of Mineral Replacement Reactions) grant PITN-GA-2008-215360. The authors thank Veronika Rapelius for help with solution preparation and ICP-OES analyses. Experimental facilities in Münster are supported by the Deutsche Forschungsgemeinschaft (DFG). L.J.W. also acknowledges funding by the Deutscher Akademischer Austauschdienst (DAAD), and a start-up grant from the Huazhong Agricultural University (52204-09008). We are thankful to two anonymous reviewers for the constructive comments that have helped us to improve the overall quality of this manuscript.

REFERENCES

Arvidson R. S., Collier M., Davis K. J., Vinson M. D., Amonette J. E. and Luttge A. (2006) Magnesium inhibition of calcite dissolution kinetics. *Geochim. Cosmochim. Acta* **70**, 583–594.

Buhmann D. and Dreybrodt W. (1987) Calcite dissolution kinetics in the system H_2O–CO_2–$CaCO_3$ with participation of foreign ions. *Chem. Geol.* **64**, 89–102.

Collins K. D., Neilson G. E. and Enderby J. E. (2007) Ions in water: characterizing the forces that control chemical processes and biological structure. *Biophys. Chem.* **128**, 95–104.

Davis K. J., Dove P. M., Wasylenki L. E. and De Yoreo J. J. (2004) Morphological consequences of differential Mg^{2+} incorporation at structurally distinct steps on calcite. *Am. Mineral.* **89**, 714–720.

De Leeuw N. H., Redfern S. E., Cooke D. J., Osguthorpe D. J. and Parker S. C. (2001) Modeling dynamic properties of mineral surfaces. *Solid–Liquid Interface Theor.* **8**, 97–112.

De Yoreo J. J., Zepeda-Ruiz L. A., Friddle R. W., Qiu S. R., Wasylenki L. E., Chernov A. A., Gilmer G. H. and Dove P. M. (2009) Rethinking classical crystal growth models through molecular scale insights: consequences of kink-limited kinetics. *Cryst. Growth Des.* **9**, 5135–5144.

Dove P. M. and Czank C. (1995) Crystal chemical controls on the dissolution kinetics of the isostructural sulfates: celestite, anglesite and barite. *Geochim. Cosmochim. Acta* **59**, 1907–1915.

Duffy D. M. and Harding J. H. (2004) Growth of polar crystal surfaces on ionized organic substrates. *Langmuir* **20**, 7637–7642.

Hay M. B., Workman R. K. and Manne S. (2003) Mechanisms of metal ion sorption on calcite: composition mapping by lateral force microscopy. *Langmuir* **19**, 3727–3740.

Koneshan S., Rasaiah J. C., Lynden-Bell R. M. and Lee S. H. (1998) Solvent structure, dynamics, and ion mobility in aqueous solutions at 25 °C. *J. Phys. Chem. B* **102**, 4193–4204.

Kowacz M. and Putnis A. (2008) The effect of specific background electrolytes on water structure and solute hydration: consequences for crystal dissolution and growth. *Geochim. Cosmochim. Acta* **72**, 4476–4487.

Lardge J. S., Duffy D. M., Gillan M. J. and Watkins M. (2010) Ab initio simulations of the interaction between water and defects on the calcite $(1\,0\,\bar{1}\,4)$ surface. *J. Phys. Chem. C.* **114**, 2664–2668.

Larsen K., Bechgaard K. and Stipp S. L. S. (2010a) The effect of the Ca^{2+} to CO_3^{2-} activity ratio on spiral growth at the calcite $\{1\,0\,\bar{1}\,4\}$ surface. *Geochim. Cosmochim. Acta* **74**, 2099–2109.

Larsen K., Bechgaard K. and Stipp S. L. S. (2010b) Modelling spiral growth at dislocations and determination of critical step lengths from pyramid geometries on calcite $\{1\,0\,\bar{1}\,4\}$ surfaces. *Geochim. Cosmochim. Acta* **74**, 558–567.

Liang Y., Baer D. R., McCoy J. M., Amonette J. E. and LaFemina J. P. (1996) Dissolution kinetics at the calcite–water interface. *Geochim. Cosmochim. Acta* **60**, 4883–4887.

Paquette J. and Reeder R. J. (1995) Relationship between surface structure, growth mechanism, and trace element incorporation in calcite. *Geochim. Cosmochim. Acta* **59**, 735–749.

Parkhurst D.L. and Appelo C.A.J. (1999) Users guide to PHREEQC (version 2) – A computer program for speciation, batch reaction, one dimensional transport, and inverse geochemical calculations. US Geological Survey Water-Resources Investigation Report 99-4259, 312pp.

Parsons D. F., Boström M., Maceina T. J., Salis A. and Ninham B. W. (2010) Why direct or reversed Hofmeister series? Interplay of hydration, non-electrostatic potentials, and ion size. *Langmuir* **26**, 3323–3328.

Piana S., Jones F. and Gale J. D. (2006) Assisted desolvation as a key kinetic step for crystal growth. *J. Am. Chem. Soc.* **128**, 13568–13574.

Pokrovsky O. S. and Schott J. (2002) Surface chemistry and dissolution kinetics of divalent metal carbonates. *Environ. Sci. Technol.* **36**, 426–432.

Raiteri P., Gale J. D., Quigley D. and Rodger P. M. (2010) Derivation of an accurate force-field for simulating the growth of calcium carbonate from aqueous solution: A new model for the calcite–water interface. *J. Phys. Chem. C* **114**, 5997–6010.

Raiteri P. and Gale J. D. (2010) Water is the key to nonclassical nucleation of amorphous calcium carbonate. *J. Am. Chem. Soc.* **132**, 17623–17634.

Rajam S. and Mann S. (1990) Selective stabilization of the (0 0 1) face of calcite in the presence of lithium. *J. Chem. Soc., Chem. Commun.*, 1789–1791.

Reeder R. J. (1996) Interaction of divalent cobalt, zinc, cadmium, and barium with the calcite surface during layer growth. *Geochim. Cosmochim. Acta* **60**, 1543–1552.

Ruiz-Agudo E., Putnis C. V., Jiménez-López C. and Rodríguez-Navarro C. (2009) An AFM study of calcite dissolution in concentrated saline solutions: the role of magnesium ions. *Geochim. Cosmochim. Acta* **73**, 3201–3217.

Ruiz-Agudo E., Kowacz M., Putnis C. V. and Putnis A. (2010) Role of background electrolytes on the kinetics and mechanism of calcite dissolution. *Geochim. Cosmochim. Acta* **74**, 1256–1267.

Stack A. G. and Grantham M. C. (2010) Growth rate of calcite steps as a function of aqueous calcium-to-carbonate ratio: independent attachment and detachment of calcium and carbonate ions. *Cryst. Growth Des.* **10**, 1409–1413.

Teng H. H., Dove P. M., Orme C. and De Yoreo J. J. (1998) Thermodynamics of calcite growth: baseline for understanding biomineral formation. *Science* **282**, 724.

Teng H. H., Dove P. M. and De Yoreo J. J. (1999) Reversed calcite morphologies induced by microscopic growth kinetics: insight into biomineralization. *Geochim. Cosmochim. Acta* **63**, 2507–2512.

Vavouraki A. I., Putnis C. V., Putnis A. and Koutsoukos P. (2008) An Atomic Force Microscopy study of the growth of calcite in the presence of sodium sulfate. *Chem. Geol.* **253**, 243–251.

Vavouraki A. I., Putnis C. V., Putnis A. and Koutsoukos P. (2010) Crystal growth and dissolution of calcite in the presence of fluoride ions: an atomic force microscopy study. *Cryst. Growth Des.* **10**, 60–69.

Weaver M. L., Qiu S. R., Hoyer J. R., Casey W. H., Nancollas G. H. and De Yoreo J. J. (2007) Inhibition of calcium oxalate monohydrate growth by citrate and the effect of the background electrolyte. *J. Cryst. Growth* **306**, 135–145.

Associate editor: George R. Helz